Laboratory Investigation (2009) 89, 178–195

Expression of galectin-1, a new component of slit diaphragm, is altered in minimal change nephrotic syndrome

Mariko Shimizu[1], Jamshid Khoshnoodi[2], Yoshihiro Akimoto[3], Hayato Kawakami[3], Hiroshi Hirano[3], Eiji Higashihara[4], Makoto Hosoyamada[5], Yuji Sekine[1], Ryota Kurayama[1], Hideaki Kurayama[6], Kensuke Joh[6], Jun Hirabayashi[7], Kenichi Kasai[8], Karl Tryggvason[9], Noriko Ito[1] and Kunimasa Yan[1]

Nephrin is an essential structural component of the glomerular slit diaphragm (SD), a highly organized intercellular junction that constitutes the ultrafiltration barrier of the kidney. Recent studies have identified two additional nephrin-interacting SD proteins (NEPH1 and NEPH2), suggesting that the zipper-like pattern of the SD is formed through complex intra- and intermolecular interactions of these proteins. However, the complexity of the SD structure suggests that additional SD components remain to be discovered. In this study, we identified galectin-1 (Gal-1) as a new component of the SD, binding to the ectodomain of nephrin. Using dual-immunofluorescence and confocal microscopy and dual-immunoelectron microscopy, we found Gal-1 colocalizing with the ectodomain of nephrin at the SD in normal human kidney. By immunoprecipitation and surface plasmon resonance, we confirmed a direct molecular interaction between Gal-1 and nephrin. Moreover, recombinant Gal-1 induced tyrosine phosphorylation of the cytoplasmic domain of nephrin and activation of the extracellular signal-regulated kinase 1/2 in podocytes. We also showed that podocytes are a major site of biosynthesis of Gal-1 in the glomerulus and that the normal expression patterns and levels of Gal-1 are altered in patients with minimal change nephrotic syndrome. Finally, in puromycin aminonucleoside-induced rat nephrosis, an apparent reduction in the levels of Gal-1 and nephrin around the onset of heavy proteinuria was also revealed. Our data present Gal-1 as a new extracellular ligand of nephrin localized at the glomerular SD, and provide further insight into the complex molecular organization, interaction, and structure of the SD, which is an active site of intracellular signaling necessary for podocyte function.

Laboratory Investigation (2009) **89,** 178–195; doi:10.1038/labinvest.2008.125; published online 15 December 2008

KEYWORDS: slit diaphragm; galectin; nephrin; podocyte; *N*-glycosylation; β-galactoside

Nephrin is a principal component of the glomerular slit diaphragm (SD), a highly specialized intercellular junction that constitutes the ultrafiltration barrier of the kidney.[1] Structurally, nephrin is a type-1 transmembrane glycoprotein with 10 predicted asparagine-(*N*)-linked glycosylation sites located on its ectodomain.[2] Recently, the sites of these *N*-linked glycans on the ectodomain of nephrin were mapped by mass spectrometry; and their terminal sugar residues were identified by the use of carbohydrate-specific lectins, which study showed that human nephrin is a sialoprotein with terminal sugars of high mannose glycans and galactose.[3] We have also shown that *N*-linked glycosylation is absolutely critical for the biosynthesis of the newly synthesized nephrin molecules in the endoplasmic reticulum (ER) and for their proper transport to the plasma membrane.[4] Moreover, we recently demonstrated that *N*-linked glycosylation of nephrin in the ER is highly dependent on the orchestration by calreticulin as a lectin chaperone and the levels of intracellular ATP as an energy source.[5,6]

[1]Department of Pediatrics, Kyorin University School of Medicine, Mitaka, Tokyo, Japan; [2]Department of Medicine, Vanderbilt University School of Medicine, Nashville, TN, USA; [3]Department of Anatomy, Kyorin University School of Medicine, Mitaka, Tokyo, Japan; [4]Department of Urology, Kyorin University School of Medicine, Mitaka, Tokyo, Japan; [5]Department of Pharmacotherapeutics, Kyoritsu University of Pharmacy, Minato-ku, Tokyo, Japan; [6]National Hospital Organization Chiba-East National Hospital, Chiba, Japan; [7]Research Center for Medical Glycoscience, National Institute of Advanced Science and Technology, Ibaraki, Japan; [8]Biological Chemistry, Faculty of Pharmaceutical Sciences, Teikyo University, Kanagawa, Japan and [9]Division of Matrix Biology, Department of Medical Biochemistry and Biophysics, Karolinska Institute, Stockholm, Sweden

Correspondence: K Yan, MD, PhD, Department of Pediatrics, Kyorin University School of Medicine, Mitaka, Tokyo 181-8611, Japan.
E-mail: kuniyan@kyorin-u.ac.jp

Received 4 May 2008; revised 7 October 2008; accepted 9 October 2008

Although the above findings underline the critical role of glycosylations in the protein folding and trafficking of nephrin, there is essentially no information on whether these glycans may play a role in the functional aspects of nephrin at the SD. In the present study, we hypothesized that galectins could be potential candidates for the extracellular ligand of nephrin. This hypothesis is based on the fact that galectins have specific affinity for β-galactosides and our recent finding that the nephrin ectodomain contains β-galactosides.[3] Galectins comprise a family of structurally related lectin proteins that, through their conserved β-galactoside recognition motif, can bind to glycoproteins and modulate a wide range of cellular activities including cell adhesion, migration, and death.[7] Of the 15 galectins so far described in mammalian tissues, galectin-1 (Gal-1), galectin-3 (Gal-3), galectin-8, and -9 have been positively identified in the kidney.[8–10] Gal-1 represents the prototype of galectins that form a homodimer and upon binding to their target molecules mediate intermolecular as well as intramolecular crosslinking.[11–13] Gal-3 represents a chimeric type of galectin that contains a single carbohydrate-binding domain followed by a collagen-like stalk that plays a role in its intermolecular association.[14] Moreover, galectin-8 and -9 represent a tandem repeat-type galectin with two carbohydrate-binding domains in the same polypeptide chain, joined by a link peptide.[9,10]

In terms of protein distribution in the mammalian kidney, galectin-9 was identified in the mouse kidney to localize in the cortical tubules, intertubular capillaries, and glomerular mesangium.[10] In the case of the transcript of galectin-8, it was identified in the rat whole kidney;[9] but no data regarding its protein distribution has been given so far. In contrast, it is well known that Gal-3 is expressed in the ureteric bud/collecting duct lineage during nephrogenesis, modulates collecting duct growth/differentiation *in vitro*, and is expressed in human autosomal recessive polycystic kidney disease in cyst epithelia, suggesting a pivotal role of Gal-3 in developmental and pathological processes in renal collecting ducts.[15] Moreover, expression and localization of Gal-1 has been controversial. In the human kidney, low expression of Gal-1 has been demonstrated in the mesangium but not in the epithelial cells of the first trimester fetus.[16] Moreover, a recent paper showed that Gal-1 was detected in podocytes in the biopsy samples from patients with diffuse mesangial proliferation and focal segmental glomerulosclerosis, whereas glomeruli from control subjects and patients with minimal change nephrotic syndrome (MCNS) were negative.[17] This interesting study suggests that alteration of Gal-1 function may be implicated in the pathomechanism of podocyte injury in acquired nephrotic syndrome and that this lectin may even play a crucial role in the maintenance of podocyte viability in the normal condition. To further explore a potential role of galectins in the biology and pathogenesis of acquired nephrotic syndrome, first we sought to determine whether human Gal-1 is present in the glomerulus of the normal kidney. In addition to Gal-1, we also examined Gal-3 expression in the glomerulus, because our previous study demonstrated that human Gal-3 was localized not only in the epithelium but also in the vascular endothelium.[18] Here we show for the first time that both Gal-1 and -3 are components of the normal glomerulus but that only Gal-1 was produced by podocytes. In addition, we show that Gal-1 is an extracellular ligand of nephrin and, thus, a new component of the glomerular SD. Moreover, we demonstrate that the expression of Gal-1 in podocytes was distinctly reduced in the human glomeruli of adult patients with MCNS and the glomeruli of rats with puromycin aminonucleoside nephrosis (PAN), whereas no apparent reduction in Gal-3 was observed in MCNS glomeruli. Finally, we show that Gal-1 induced tyrosine phosphorylation of the intracellular domain of nephrin, which rapidly resulted in an increased phosphorylation and activation of the extracellular signal-regulated MAP kinase (ERK) 1/2.

MATERIALS AND METHODS

Antibodies and Recombinant Proteins

Mouse monoclonal (mAb2) and rabbit polyclonal (pAb2) antibodies against human nephrin were previously described.[4–6,19] Rabbit polyclonal anti-human Gal-1 was generated against dimeric Gal-1 and purified by asialofetuin-Sepharose affinity column from human placenta.[12,13] Rabbit polyclonal anti-human Gal-3 was previously described.[18] Mouse monoclonal anti-podocalyxin antibody was kindly donated by Dr M Hara (Yoshida Hospital, Niigata, Japan) and reported previously.[20] The following antibodies were purchased from the suppliers indicated: anti-laminin α5 monoclonal antibody (clone 4C7; Chemicon International Inc., Temecula, CA, USA), anti-synaptopodin monoclonal antibody (PROGEN, Heidelberg Germany), anti-mouse Gal-1 goat polyclonal antibody (R&D systems, Minneapolis, MN, USA), anti-phosphotyrosine (PY20) monoclonal antibody (Becton Dickson Transduction Laboratories, Franklin Lakes, NJ, USA), polyclonal antibodies against ERK1/2 and phospho-ERK1/2 (Cell Signaling Technology, Beverly, MA, USA), anti-β-actin monoclonal antibody (Sigma-Aldrich, St Louis, MO, USA); Texas Red-X goat anti-mouse IgG, Alexa Fluor 488-conjugated goat anti-rabbit IgG and Alexa Fluor 488-conjugated donkey anti-goat IgG, (Molecular Probes, Eugene, OR, USA); horseradish peroxidase (HRP)-labeled goat anti-mouse and anti-rabbit immunoglobulins (Dako, Kyoto, Japan). A recombinant soluble histidine-tagged nephrin (NPH-His),[3,21] wild-type galectin-1 (WT Gal-1) and mutant C2S (MU Gal-1) human recombinant galectin-1[12,22] were described previously.

Kidney Samples and Isolation of Glomeruli

Samples of human kidney cortex were obtained from histologically normal regions of fresh kidneys from patients undergoing nephrectomy with renal cancer or ureter cancer at the Department of Urology, Kyorin University School of Medicine, as previously described.[23–25] Isolation of human

Table 1 Kinetic rate constants for interaction of Gal-1 (MU Gal-1) to nephrin

R_{max} (RU)	χ^2	k_{a1} (M/s)	k_{d1} (per s)	K_{D1} (μM)	k_{a2} (per s)	k_{d2} (per s)	K_{D2}
350 ± 0.1	7.8	569 400 ± 71 000	0.989 ± 0.055	1.7 ± 0.1	2359 ± 25.6	0.0038 ± 0.000	1.6 ± 0.01

The sensorgrams were best fitted into a 1:1 interaction model with conformational change. This type of interaction is defined by two association (k_{a1}, k_{a2}) and two dissociation (k_{d1}, k_{d2}) rate constants as described in the table. The second equilibrium dissociation constant (K_{D2}) is unit-less. Maximum response (R_{max}) and the χ^2-value showing the statistically significant curve fit are indicated.

glomeruli was performed by a differential sieving technique.[23–25] Informed consent was obtained from all of the patients. Fresh kidney samples of rodents were obtained from male ICR mice and Sprague–Dawley strain rats (Saitama Experimental Animals Supply Co., LTD, Sugito, Saitama, Japan). Isolation of mouse and rat glomeruli was performed by the magnetic beads method.[26]

Human Podocyte Cell Line Culture

The human SV40-transformed podocyte cell line (T-SV40-GE), a kind gift from Dr Jean-Daniel Sraer at Hospital Tenon, Paris, was cultured and maintained as previously described.[27] Although the expression of human nephrin in T-SV40-GE cells was detectable by reverse transcription (RT)–PCR (data not shown), proper detection of endogenous nephrin protein by immunostaining and western blotting was not satisfactory. Thus, we transiently transfected the cell line with a human full-length nephrin construct described previously.[4–6] T-SV40-GE cells were transiently transfected with a plasmid expression vector encoding the full-length human nephrin or the vector alone. After 48 h, the medium was replaced with serum-free medium containing or lacking recombinant wild-type Gal-1 (5 μg/ml); and the cells were then harvested at various times up to 6 h and subjected to immunoprecipitation and Western blot analysis with phosphotyrosine, ERK1/2, and phospho-ERK1/2.

Puromycin Aminonucleoside Nephrosis

Puromycin aminonucleoside nephrosis was established as previously described.[28] Kidney cortex was obtained from rats at day 0–5 rat after the injection of PAN and examined immunohistochemically as described below. Protein lysates was obtained from isolated glomeruli and analyzed for protein expression of Gal-1, nephrin and β-actin. Urine (10 μl) was loaded onto a 5–20% gradient gel for SDS–polyacrylamide gel electrophoresis (PAGE), electrophoresed, and stained with Coomassie blue. The amounts of urinary protein excretion and creatinine were measured by the Bradford method (Bio-Rad, Oakland, CA, USA) and the Jaffe assay, respectively.

Patients and Renal Biopsies

Indirect immunohistochemistry was performed on paraffin-embedded sections of archival renal biopsies at the National Hospital Organization Chiba-East National Hospital. Samples from eight adult cases of clinically and morphologically typical MCNS and six samples from patients with minor glomerular abnormalities (MGA) who had solitary glomerular hematuria or hematuria combined with mild proteinuria (Table 1) were selected for Gal-1 and -3 staining as described below. All samples were fixed with 20% formaldehyde-phosphate-buffered saline (PBS) overnight at room temperature and embedded in paraffin wax. All patients showed the normal range glomerular function and had not been treated with glucocorticoid therapy. Informed consent was obtained from all patients.

Immunohistochemistry

Samples of normal human kidney cortex were fixed in 10% formaldehyde in PBS for 6 h at 4°C, embedded in paraffin wax, and sectioned at a 4-μm thickness. The slides were dewaxed, washed with PBS, and autoclave heated at 120°C for 10 min in Target Retrieval Solution (Dako) for antigen retrieval. After incubation with 1% H_2O_2/PBS for 30 min and washing with PBS, the slides were incubated with blocking buffer (3% BSA, 5% goat serum, and 0.05% Tween-20 in PBS) for 60 min, and then reacted with anti-Gal-1 antiserum, anti-Gal-3 antiserum, or preimmune rabbit serum (1:2000, respectively) for 60 min at room temperature. After washing with PBS, the slides were incubated at room temperature with HRP-labeled goat anti-rabbit antibody (1:100), and then developed by immersion in 1.4 mM 3,3′-diaminobentizine tetrahydrochloride (Sigma) in PBS. Archival renal biopsy samples were fixed in 20% formaldehyde PBS overnight at room temperature and embedded in paraffin wax. Sections of 2-μm thickness were prepared, autoclave heated, and then immunostained for Gal-1 and -3 as above. Immunostaining and label intensity score of Gal-1 and -3 sections were evaluated by three independent reviewers. A total of 10 glomeruli were evaluated at low-power magnification to assess the labeling intensity of whole glomeruli. The reviewers' scores were averaged and expressed from high (+++) to negligible (0). Kidney samples from mouse and rat were fixed in 10% formaldehyde PBS overnight at room temperature, and embedded in paraffin. After autoclave heating as above, the slides were reacted with anti-Gal-1 antibody (10 μg/ml) overnight at 4°C, incubated with secondary antibody, and developed as mentioned above.

Immunoelectron Microscopy

Samples of human normal kidney cortex were fixed in 4% paraformaldehyde PBS for 6 h at 4°C and embedded in LR gold resin (Polysciences Inc., Warrington, PA, USA).

Ultrathin sections were picked up on electron-microscopic grids coated with a formvar membrane. They were first placed on a drop of PBS for 10 min and then transferred to a drop of 1% BSA-5% normal donkey serum PBS and kept there for 10 min. The grids were then transferred to a drop of anti-Gal-1 (1:2000) and/or anti-nephrin antibody (mAb2, 5 μg/ml), incubated for 1 h, rinsed with PBS, and reacted with colloidal gold (12 nm in diameter for Gal-1)-conjugated anti-rabbit IgG diluted at 1:20 or colloidal gold (18 nm in diameter for nephrin)-conjugated anti-mouse IgG diluted at 1:20 for 1 h in a moist chamber. The grids were then rinsed with PBS followed by distilled water. The sections were stained with uranyl acetate for 30 s, and then examined under an electron microscope (JEM-1010; JEOL, Tokyo Japan). To quantify the ratio of colocalization of Gal-1 and nephrin, we counted immunogold particles of each size in 50 fields of the SD.

Immunofluorescence and Confocal Microscopy

For the dual immunostaining of Gal-1 and laminin-α5 or nephrin, human kidney cortex was fixed in 4% paraformaldehyde PBS for 6 h at 4°C; immersed sequentially in 5, 10, and 20% sucrose PBS; and embedded in OCT compound. The frozen sections were incubated with blocking buffer for 1 h at room temperature. The sections were then reacted with the primary antibodies, Gal-1 (1:2000) and laminin-α5 (1:500) or nephrin (mAb2, 5 μg/ml), for 1 h at room temperature. Immunocomplexes were visualized by using Alexa Fluor 488-conjugated goat anti-rabbit IgG (5 μg/ml) and Texas Red-X goat anti-mouse IgG (5 μg/ml), respectively. Fresh frozen sections of the kidney cortex from rats with PAN nephrosis were incubated with anti-nephrin antibody (pA2). For synaptopodin immunostaining, fresh frozen sections were fixed with 4% paraformaldehyde for 10 min. The primary antibodies were reacted overnight at 4°C, and then immunocomplex was visualized by using Alexa Fluor 488-conjugated goat anti-rabbit IgG and Texas Red-X goat anti-mouse IgG, respectively. Slides were examined under a confocal laser-scanning microscope equipped with a Krypton/Argon laser (MRC1024, Bio-Rad).

Co-immunoprecipitation

The crude membrane fraction from human glomeruli was obtained by using lysis buffer.[6,23] After centrifugation to remove insoluble materials, the supernatants were incubated with protein A-Sepharose CL-4B (Amersham) for 1 h at 4°C to rid the lysates of proteins that nonspecifically bind to protein A-Sepharose beads. The supernatants were incubated with anti-nephrin antibody (pAb2) and anti-podocalyxin antibody for 1 h at 4°C. The immunocomplex of the supernatant and anti-podocalyxin antibody was further incubated with rabbit IgG against mouse IgG for 1 h at 4°C. Samples were then further incubated with protein A-Sepharose CL-4B for 1 h at 4°C. The pellets of Sepharose beads were washed four times with lysis buffer and then used for western blot analysis for nephrin and Gal-1. T-SV40-GE cells transfected with nephrin cDNA were incubated with recombinant Gal-1 (5 μg/ml) for 1 h. The crude membrane fraction was obtained by using lysis buffer. After the supernatants had been incubated with protein A-Sepharose CL-4B as above, the supernatants were incubated with anti-nephrin antibody (pAb2) for 1 h at 4°C, and then further incubated with protein A-Sepharose CL-4B for 1 h at 4°C. The pellets of Sepharose beads were washed four times with lysis buffer, and then immunoprecipitate and total lysates were used for western blot analysis for nephrin, PY-20, ERK1/2, and phospho-ERK1/2.

Western Blot Analysis

Samples were separated by 15% or 5–20% gradient SDS–PAGE under reducing conditions and transferred to polyvinilidene difluoride membranes. Blots were incubated with primary antibodies: anti-nephrin (mAb2: 0.5 μg/ml), anti-human Gal-1 (1:10000), anti-human Gal-3 (1:5000), anti-PY20 (1 μg/ml), anti-ERK1/2 (1:1000), anti-phospho-ERK1/2 (1:1000), preimmune rabbit serum (1:5000), anti-mouse Gal-1 (0.1 μg/ml), or goat IgG (0.1 μg/ml) for 1 h at room temperature. All blots were incubated with appropriate secondary antibody and detected by using a chemiluminescent kit (PerkinElmer Life Sciences, Boston, MA, USA) according to the manufacturer's instructions.

Reverse Transcription–PCR

Total RNA was extracted from isolated human glomeruli and T-SV40-GE cells by using Isogen (Wako Life Science Reagents, Osaka, Japan). Total RNA (1 μg) was amplified by using a Gene Amp PCR core kit and specific primer sets against human Gal-1 (accession no.: NM_002305; sense primer, 5′-AACCTGGAGAGTGCCTTCGA-3′; antisense primer, 5′-GTAGTTGATGGCCTCCAGGT-3′). Amplification was carried out under the following conditions: 25 cycles at 94°C for 1 min, 58°C for 1 min and 72°C for 2 min; and PCR products were analyzed by electrophoresis on 1% agarose gels, followed by direct sequencing to confirm the correct product.

Surface Plasmon Resonance and Protein Interaction Analysis

Binding analysis based on surface plasmon resonance (SPR) using a BIAcore 2000 optical biosensor (GE Healthcare, Uppsala, Sweden) was conducted. Interactions were measured in resonance units (RUs) in which 1 RU is equal to 1 pg/mm^2 bound protein. All proteins were dialyzed against running buffer, TBST-EDTA (10 mM Tris, 0.15 M NaCl, 0.005% surfactant Tween-20, 3.0 mM EDTA; pH 7.4). Purified Neph-His and BSA as control were diluted in immobilization buffer (10 mM Na-acetate buffer, pH 5.0 for nephrin, or pH 4.0 for BSA) to a final concentration of 20 μg/ml and immobilized in equivalent molar ratios. Amine-coupling chemistry was used to immobilize the ligand proteins on carboxymethylated dextran surfaces of CM5

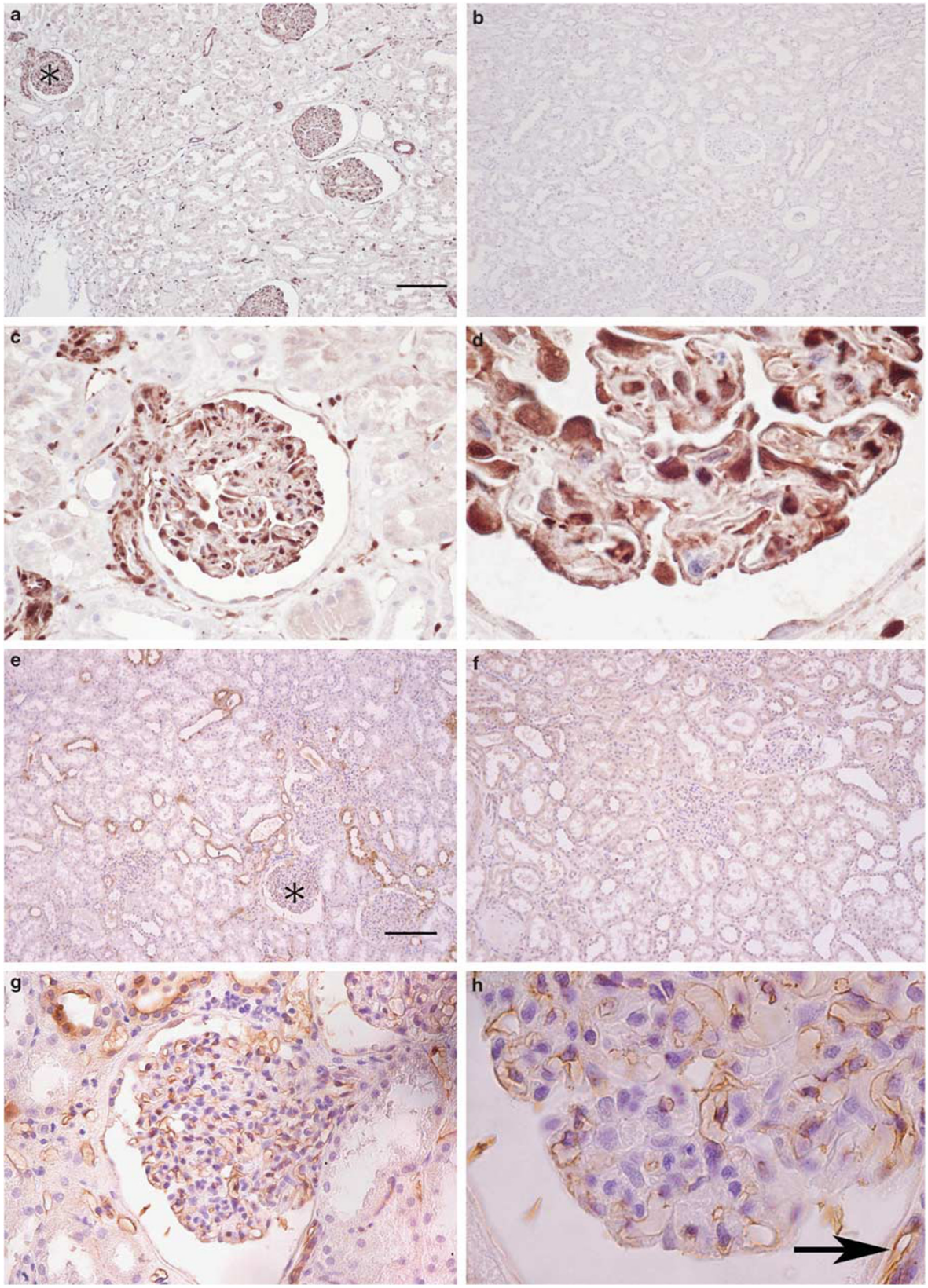
a
b
c
d
e
f
g
h

research-grade sensor chips (GE Healthcare). The flow cell surfaces were activated by injecting a 1:1 mixture of 0.05 M *N*-hydroxysuccinimide and 0.2 M 3-(*N*,*N*-dimethylamino) propyl-*N*-ethylcarbodi-imide at a flow rate of 20 μl/min at 25°C for 10 min. For immobilization, ligands were injected at a flow rate of 5 μl/min. Equal molar surface densities of Neph-His (~2900 RU) and BSA (~1200 RU) as a reference were generated. Signals from the BSA surface were used as negative control for background subtractions. A third flow cell was treated only with activation and blocking solutions and was used as a blank surface for buffer subtraction. After immobilization, the remaining reactive esters on the carboxymethyl-dextran surfaces were blocked with 1 M ethanolamine (pH 8.0). All interactions were performed at the flow rate of 20 μl/min and room temperature (22°C). Analyte samples were diluted in the running buffer and injected in triplicate at different concentrations (0.25, 0.5, 1.0, 2.0, and 4.0 μM). Interactions were performed with a contact time of 180 s followed by a dissociation phase of an equal time. After each cycle, the surfaces were regenerated by two subsequent injections of 40 μl of 1 M ethanolamine (pH 8.4), followed by equilibration with the running buffer for 10 min.

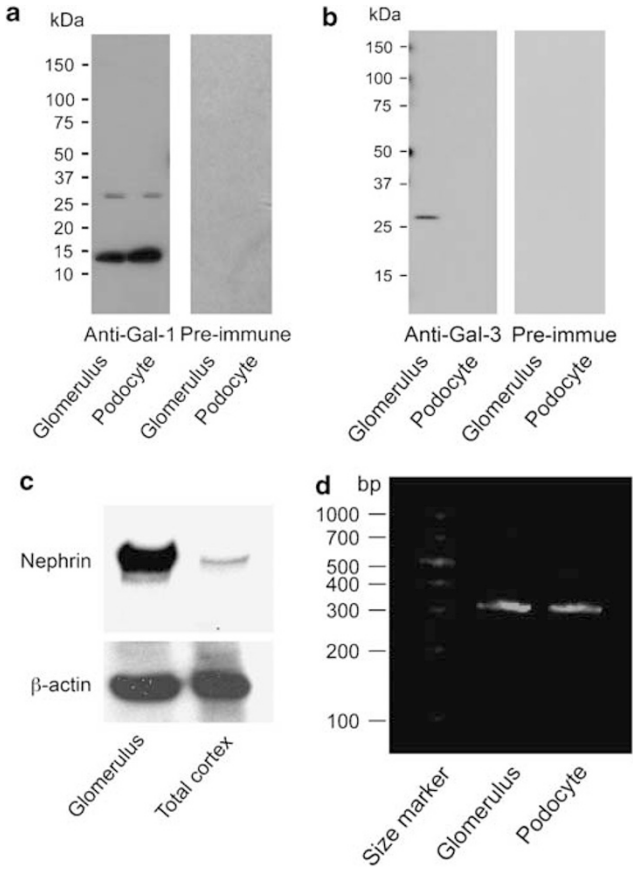

Figure 2 Expression of Gal-1 and -3 in the human glomerulus and cultured podocytes. (**a**) Western blot analysis detected a 14-kDa monomer and a 28-kDa dimer form of Gal-1 in 10 μg of the protein extracts of isolated human glomerulus and cultured podocytes. (**b**) Western blot analysis detected a 30-kDa protein band of Gal-3 in the same samples of (**a**). (**c**) Western blot analysis with nephrin in the glomerular sample used in (**a**) and (**b**) revealed strong upper band, plasma membrane form, and faint under band, ER form, whereas its expression was detected to be very faint in the total cortex sample. (**d**) Specific expression of Gal-1 at the transcript level can also be demonstrated by RT–PCR of isolated mRNA from glomeruli and cultured podocytes using specific primers corresponding to a 323-bp long internal sequence of human Gal-1 cDNA.

Data Analysis and Determination of Kinetic Constants

All data processing including scale transformation and background and reference subtractions were performed by using BIAevaluation 3.0. (GE Healthcare). Data evaluation and calculations based on numerical approaches including global curve fitting to interaction models and calculation of kinetic constants were performed with IGOR Pro software (version 4.01.A, WaveMetrics Inc., Lake Oswego, OR, USA). Global curve-fit calculations were performed with fixed values for the constant parameters M_w, h_{diff}, and k_c; whereas the global parameters k_a, k_d, and R_{max} were defined as free-running parameters to be determined by the global fit routine, as described before.[21,29] The local parameter C_A (analyte monomer concentration) was also defined as a free-running variable with constraints within the range of total analyte concentration.

RESULTS

Expression and Localization of Gal-1 and Gal-3 in Human Glomerulus

As shown in Figure 1, a strong and specific immunostaining for Gal-1 could be detected in the glomerulus and the interstitial area (Figure 1a and c). Higher magnification of the glomerulus revealed that Gal-1 was strongly expressed in the capillary tuft, nucleus, and cytoplasm of podocytes and endothelial cells, and moderately expressed in mesangial cells and Bowman's epithelium (Figure 1c and d). Gal-1 was also detected in the fibroblasts located in the interstitial area (Figure 1c), whereas preimmune serum did not show any reactivity (Figure 1b). The expression of Gal-3, moreover, was strongest in the collecting ducts (Figure 1e and g); however, some immunostaining was also detected in the

Figure 1 Immunohistochemistry of Gal-1 and -3 in human kidney. (**a**) Low magnification revealed positive immunostaining of Gal-1 in the glomerulus (asterisk) and the interstitial area. (**c**, **d**) High-power magnification from asterisk in (**a**) showed Gal-1 to be strongly expressed in the podocytes, endothelium and the capillary walls, moderately in mesangial cells and Bowman's epithelium. Gal-1 was also localized in the interstitial fibroblast. (**e**) Low magnification detected Gal-3 to be strongly expressed in the collecting ducts and weakly in the glomerulus (asterisk). (**g**, **h**) Gal-3 (asterisk in **e**) was expressed in the glomerular endothelium as well as capillary endothelium (arrow). (**b**, **f**) Preimmune serum showed no reactivity to kidney sections, indicating the specificity of the anti-Gal-1 and Gal-3 antibodies. Size bars are 100 μm in (**a**) and (**e**).

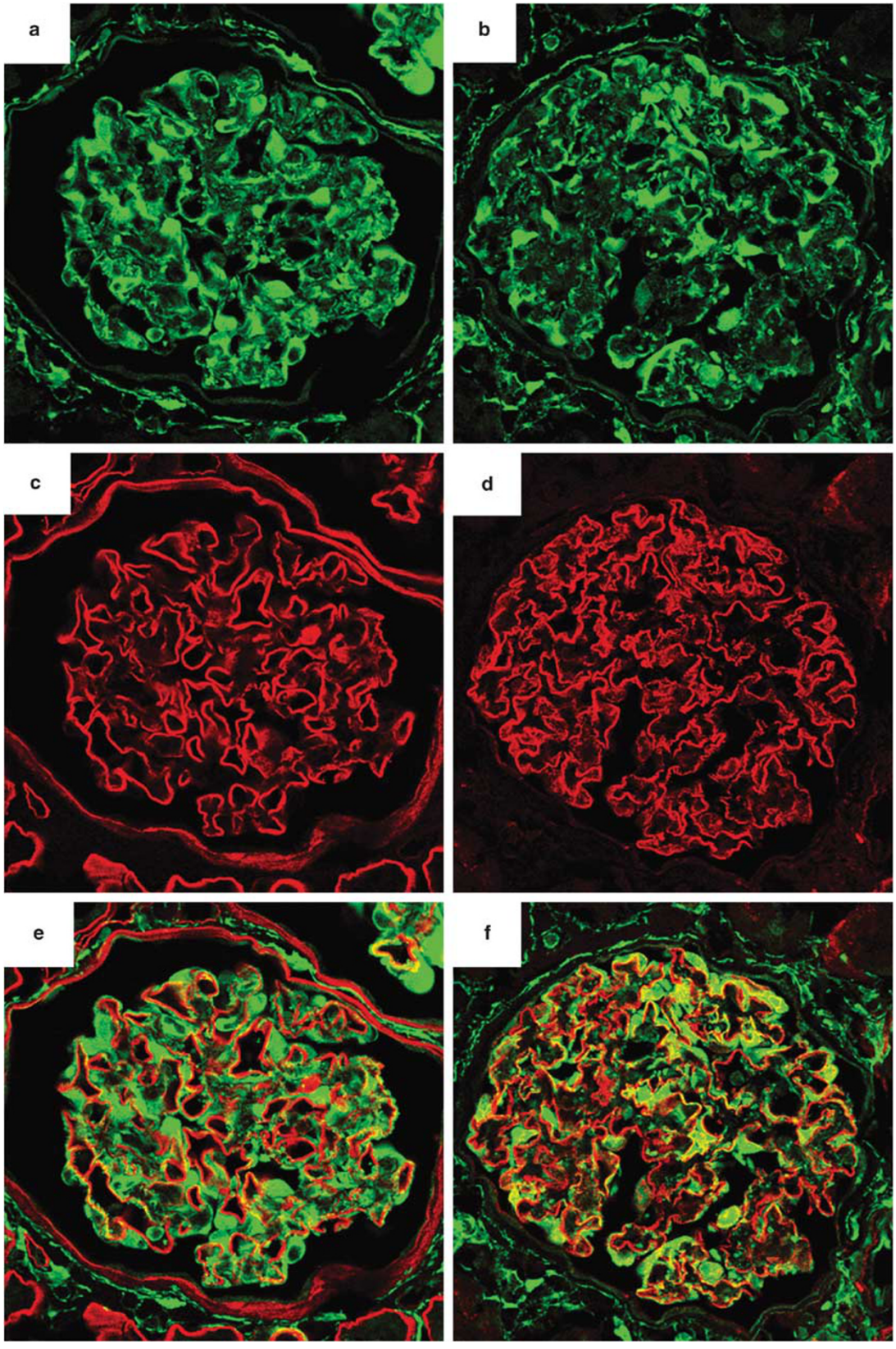

Figure 3 Subcellular localization of Gal-1 with laminin 11 and nephrin in the human glomerulus. Dual immunofluorescence and confocal microscopy showed the colocalization of Gal-1 (**a**, **b**) with laminin α5 chain (**c**) and nephrin (**d**) as shown by merged images in (**e**) and (**f**), respectively.

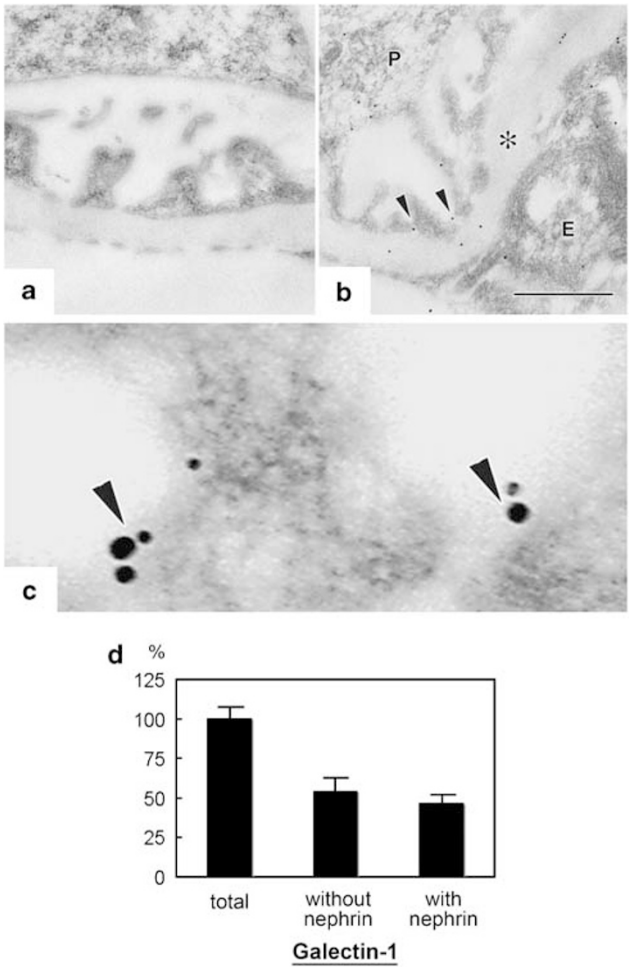

Figure 4 Immunoelectron microscopy of Gal-1 in the human glomerulus. (**a**) Preimmune serum showed no reactivity. (**b**) Immunogold particles directed to Gal-1 showed the localization of Gal-1 in the podocyte cytoplasm (P), endothelial cell (E) and the GBM (asterisk) and between the podocyte foot processes (arrow heads). (**c**) A higher magnification of the double-labeled immunogold section clearly showed the colocalization of Gal-1 (12-nm gold particle) and nephrin (18-nm gold particle) at the podocyte SD (arrow heads). Size bars in (**b**) (500 nm) was indicated. (**d**) Quantification of the ratio of colocalization of Gal-1 and nephrin in (**c**) were counted in the 50 fields at the SD.

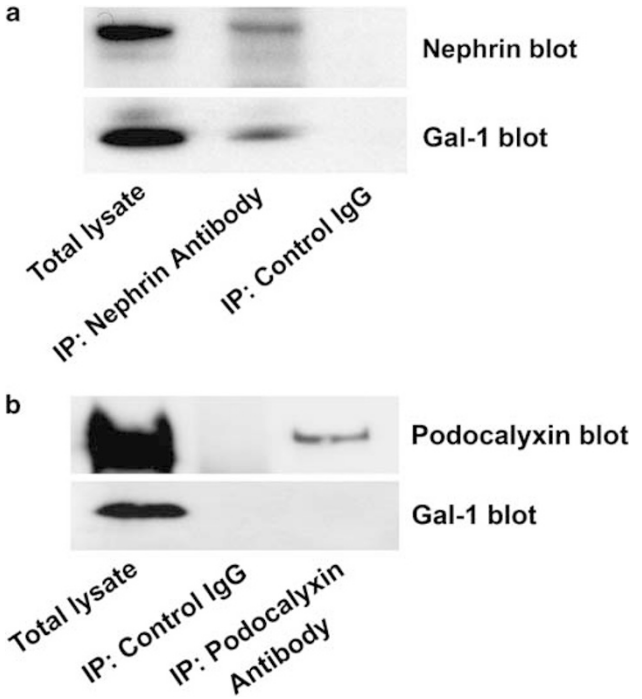

Figure 5 Co-immunoprecipitation of Gal-1. Immunocomplexes were precipitated using antibody against nephrin and podocalyxin, separated on SDS–PAGE gels and blotted on membranes. Gal-1 was pulled down by nephrin from the protein extracts of human glomeruli (**a**), but not by podocalyxin (**b**).

glomerulus (Figure 1e). Higher magnification of the glomerulus showed that, contrary to the Gal-1 distribution, Gal-3 was localized only in the glomerular endothelium (Figure 1g and h) and interstitial endothelium (Figure 1h, arrow). No podocyte pattern was detected for Gal-3 and preimmune serum did not show any reactivity (Figure 1f).

Western blot analysis clearly detected Gal-1 to be a 14-kDa protein in the samples from isolated human glomeruli and cultured human podocytes (T-SV40-GE; Figure 2a). A minor fraction of Gal-1 was also seen as a 28-kDa protein band, probably corresponding to its dimer form. Gal-3, moreover, could be detected only in the glomerular sample migrating as a 30-kDa protein (Figure 2b). Figure 2c shows abundant nephrin in the glomerular sample; whereas its faint expression was observed in the total kidney cortex, indicating the credibility of the protein samples and actual existence of Gal-1 and -3 in the human glomerulus. In addition, RT–PCR of total RNA from isolated glomeruli and cultured podocyte detected a specific 323-bp cDNA fragment corresponding to the human *Gal-1* gene (Figure 2d). The PCR primers were designed to be specific for consecutive exons flanked by an intron, assuring that the 323-bp PCR fragment was not derived from the genomic DNA. Direct sequence analysis of these PCR fragments further confirmed the identity of the DNA fragment (data not shown).

Colocalization of Gal-1 with Laminin and Nephrin in the Glomerulus

Being interested in a potential interaction of Gal-1 with *N*-linked glycans of nephrin at the SD, we further investigated the subcellular localization of Gal-1 in the human glomerulus by using dual immunofluorescence and confocal microscopy. As laminin is known to be an extracellular ligand of Gal-1,[30] we examined the relative localization of Gal-1 with respect to the glomerular basement membrane (GBM). As shown in Figure 3, in addition to the podocyte cell body, endothelial cells, and mesangial cells, the GBM also showed partial but clear colocalization of Gal-1 with laminin 11 (Figure 3a, c and e). More interestingly, a partial, but nonetheless, clear colocalization of Gal-1 with

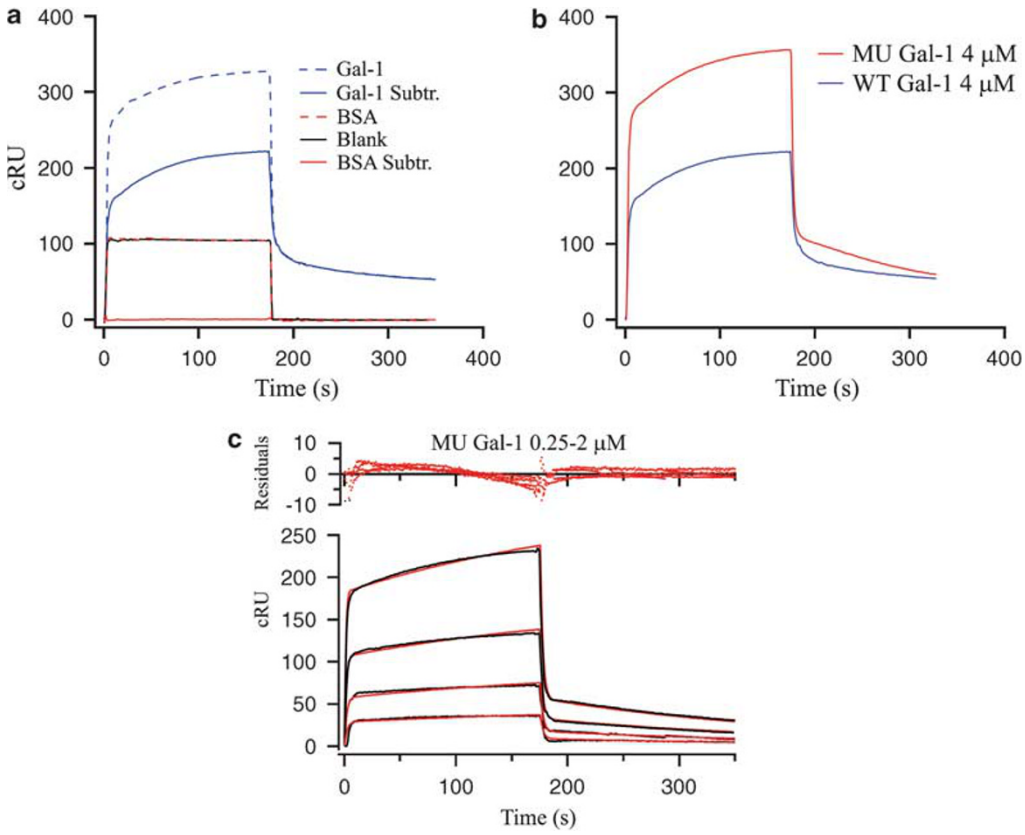

Figure 6 Surface plasmon resonance sensorgrams of Gal-1 and nephrin interactions. (**a**) The specific binding response of Gal-1 (4 μM) injected over immobilized nephrin. The blue solid line (Gal-1 Subtr.) represents the corrected response units (cRU) obtained after subtraction of the nonspecific signal recorded from the BSA surface (dotted red line) and subtraction of the blank surface (black solid line) as the background buffer response. (**b**) Binding comparison of the wild-type (WT Gal-1) and C2S mutant Gal-1 (MU Gal-1) to immobilized nephrin. Both samples were injected at equal concentration (4 μM). (**c**) Global curve-fit analysis of sensorgrams for interaction of C2S mutant (MU Gal-1) injected at different concentrations (0.25, 0.5, 1, 2 μM) over an immobilized surface of nephrin. Sensorgrams are shown in black and the global curve fits are shown in red. The goodness of curve fits is shown as residual plots above each sensorgram.

nephrin was also detected in the glomerulus (Figure 3b, d and f). To further confirm these colocalizations, we next employed immunoelectron microscopy for Gal-1 and nephrin in human kidney sections. As expected, Gal-1 was clearly localized in the endothelial cells, podocyte cytoplasm, the GBM, and the SD (arrowhead, Figure 4b) whereas no positive labeling was observed in the samples reacted with rabbit serum (Figure 4a). In addition, dual labeling for Gal-1 and nephrin clearly determined that both molecules were also colocalized at the SD (Figure 4c). Quantification of immunogold particles that labeled both nephrin and Gal-1 was also conducted. In the 50 SD fields, about 50% of the Gal-1 particles at the SD had colocalized with nephrin (Figure 4d), raising the possibility that Gal-1 could directly interact with nephrin at the SD.

Direct Interaction of Gal-1 with Nephrin

Using nephrin as molecular bait, we first performed a pull-down assay to examine a potential molecular interaction between Gal-1 and nephrin. Gal-1 was successfully pulled down by nephrin antibody from cell lysates of human isolated glomerulus (Figure 5a). To confirm specific interaction of Gal-1 with nephrin, we also performed a pull-down assay with podocalyxin, another glycoprotein expressed in podocyte.[20] As shown in Figure 5b, Gal-1 was not pulled down by the podocalyxin antibody. This prompted us to further investigate the nephrin-Gal-1 interaction by SPR technology, which provides direct measurement of molecular interactions and kinetics of binding. To ensure proper glycosylation of nephrin, we used a previously reported human embryonic kidney cell line (HEK293), stably expressing a cDNA construct encoding the entire ectodomain of human nephrin.[21] The sites of *N*-linked glycans and their terminal sugars in the recombinant nephrin were previously characterized by mass spectrometry and the use of specific lectins, respectively, which study demonstrated that the ectodomain of human nephrin contains sialic acid, high mannose glycans, and β-galactose.[3] As for Gal-1, we used a human recombinant WT Gal-1[12] and a mutated form (MU Gal-1)[22] in our studies. It has been reported that MU Gal-1 is highly stable in solutions as apposed to WT Gal-1.[22] In a series of binding studies, the recombinant nephrin was immobilized on carboxymethylated dextran surfaces of a sensor chip as the

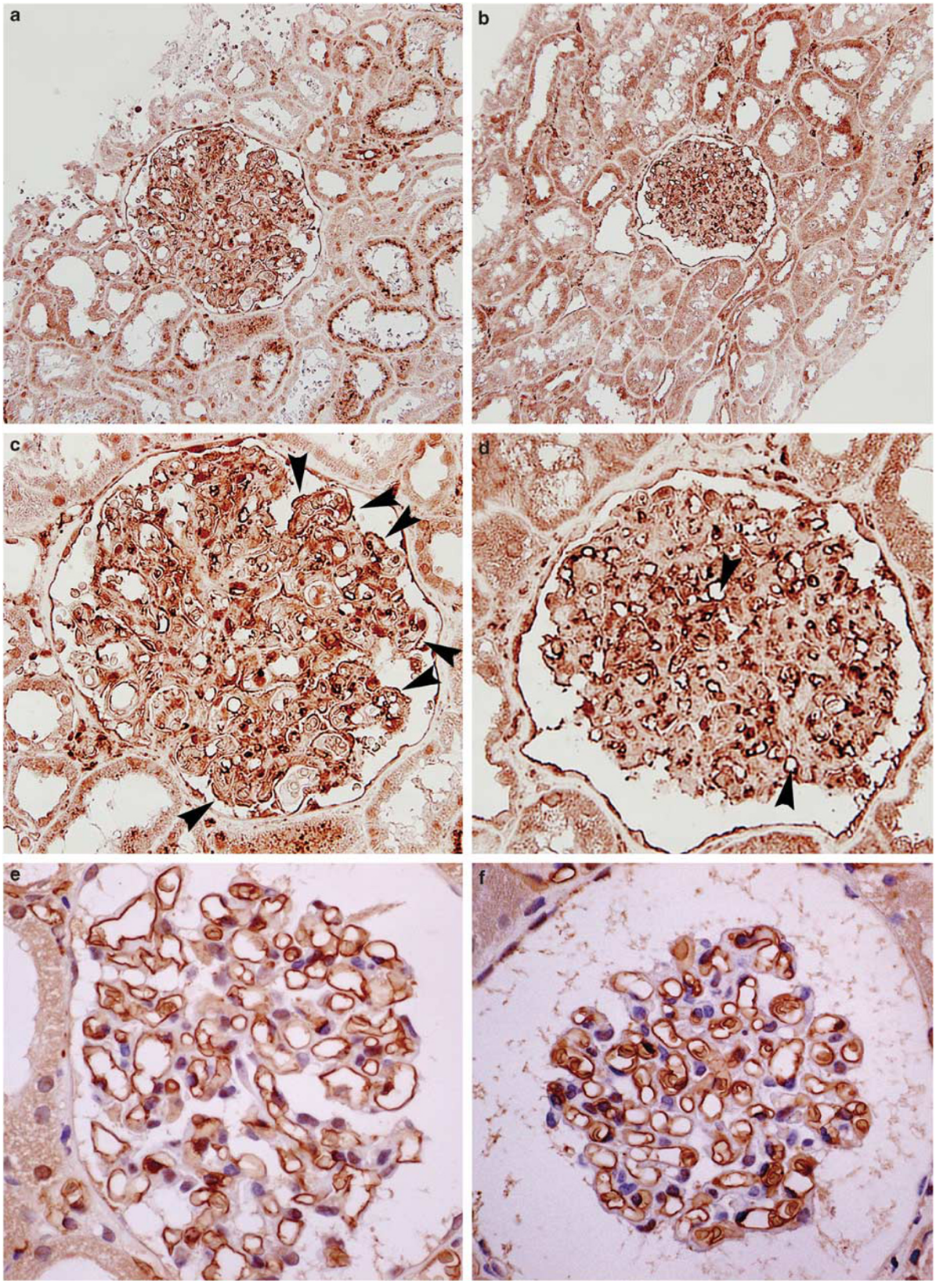

Figure 7 Representative protein distribution of Gal-1 and -3 in the glomerulus with minor glomerular abnormality (MGA; **a**, **c**, **e**) and minimal change nephrotic syndrome (MCNS; **b**, **d**, **f**). Paraffin-embedded kidney biopsy specimens were subjected to immunohistochemistry and development was performed at the same time. Gal-1 was apparently detected in the capillary tufts in MGA glomerulus (**c**, arrow head), whereas Gal-1 in the MCNS glomerulus was rather found in the endothelium not in the capillary tufts (**d**, arrow head). Moreover, there was no apparent reduction of Gal-3 immunostaining between MGA and MCNS glomeruli.

Table 2 Relation between urine protein and glomerular staining of galectin-1 and galectin-3 in the patients with minor glomerular abnormality and MCNS

Gender (age)	Urine protein (g/day)	Galectin-1	Galectin-3
MGA			
1. Female (25)	0.0	+++	++
2. Male (42)	0.8	++	+++
3. Female (36)	0.0	+++	+++
4. Male (59)	0.3	+++	+++
5. Female (22)	0.1	++	+++
6. Female (19)	0.0	+++	+++
MCNS			
1. Female (38)	4.4	+	++
2. Female (25)	3.5	+	+++
3. Male (55)	4.5	+	+++
4. Male (64)	12.0	±	+++
5. Female (33)	3.8	+	+++
6. Female (52)	4.3	±	+++
7. Male (27)	10.1	+	+++
8. F, (56)	3.2	±	+++

MGA, minor glomerular abnormalities; MCNS, minimal change nephrotic syndrome.

ligand, and WT Gal-1 was injected as the analyte. Figure 6a shows a strong and specific binding response between WT Gal-1 and nephrin after subtracting the unspecific background signal from the reference BSA surface. We next examined the differences between WT Gal-1 and MU Gal-1 in terms of binding affinity and specificity to nephrin. When equal concentrations of WT Gal-1 and MU Gal-1 were injected over the immobilized nephrin surface, a significantly higher binding signal (over 60%) was recorded for MU Gal-1 relative to WT Gal-1 (Figure 6b). The association and dissociation phases for both interactions were biphasic, indicating that the intermolecular association and dissociation occurred at two stages, a rapid initial rate (k_{a1} and k_{d1}), followed by a slower rate (k_{a2} and k_{d2}). The relatively higher binding signal of the MU Gal-1 is most likely attributed to the higher stability of the mutant, rather than higher binding affinity, as shown by the overall very similar association and dissociation profiles between the MU Gal-1 and WT Gal-1. Interestingly, this higher molecular stability of the mutant was also noted in the somewhat slower secondary dissociation rate (k_{d2}) as indicated in the last phase of the dissociation phase (Figure 6b).

We next studied the kinetics of interaction by injecting different concentrations (0.25, 0.5, 1.0, and 2.0 μM) of WT Gal-1 and MU Gal-1 onto immobilized nephrin. As expected, the analysis of the sensorgrams revealed a concentration-dependent binding for both forms of Gal-1 (Figure 6c, data shown only for the MU Gal-1). Using global curve-fit analysis, we found that the bimolecular interaction of Gal-1 and nephrin could be best fitted to a simple 1:1 interaction with conformational change and that the kinetic constants could be calculated. As shown in Table 1, the first association rate constant (k_{a1}) for this interaction showed a $\sim$240-fold higher rate than the second association rate constant (k_{a2}), clearly indicating a fast initial interaction followed by a slower one, as noted from the sensorgram profile (Figure 6c). Similarly, the same magnitude ($\sim$260-fold) of difference was also found between the first (k_{d1}) and second (k_{d2}) dissociation rate constants, indicating that the initial dissociation occurred with a much higher rate (Table 1). Taken together, from these kinetic studies, we could calculate an equilibrium dissociation constant ($K_D = 1.7$) in the lower μM range, indicating a moderate affinity for the interaction of Gal-1 and the nephrin ectodomain.

Glomerular Expression of Gal-1 is Reduced in MCNS

A recent study found that the intensity of Gal-1 immunostaining is reduced in the glomerulus of child cases with MCNS.[17] In the present study, by using our antibody, we also investigated the expression pattern of Gal-1 in the kidney sections of adult patients with MCNS before the glucocorticoid treatment. Paraffin-embedded sections of archival kidney biopsy samples from patients with either MCNS ($N = 8$) or MGA ($N = 6$) were immunostained for Gal-1. This examination revealed that the majority of MCNS glomeruli had a significantly lower expression of Gal-1, especially in the area of the glomerular tufts, than the control glomeruli from individuals with MGA (Figure 7a-d, Table 2). As a point of reference, we also studied the expression of Gal-3 in the same set of samples. However, in contrast to Gal-1, the Gal-3 expression showed no significant change between normal and MCNS (Figure 7e and f, Table 2).

Difference in Distribution of Gal-1 between Glomeruli from Different Rodents

The above findings suggest that the reduction in Gal-1 expression in the podocytes of patients with MCNS might be involved in the pathogenesis of nephrotic syndrome. However, a previous study showed no apparent proteinuria in the Gal-1-deficient mice.[31] To address this contradictory observation, we investigated Gal-1 expression and localization in two rodent species, the rat and the mouse. In the rat glomerulus, Gal-1 showed a pattern similar to that in the human kidney; ie, it was strongly expressed in podocytes, endothelium, and Bowman's epithelium, but moderately expressed in the capillary tuft and mesangial cells (Figure 8a). However, in the mouse glomerulus, Gal-1 expression was present mainly in the mesangial cells and Bowman's epithelium, and almost absent in the podocytes and capillary tuft (Figure 8b). Goat serum used instead of primary antibody

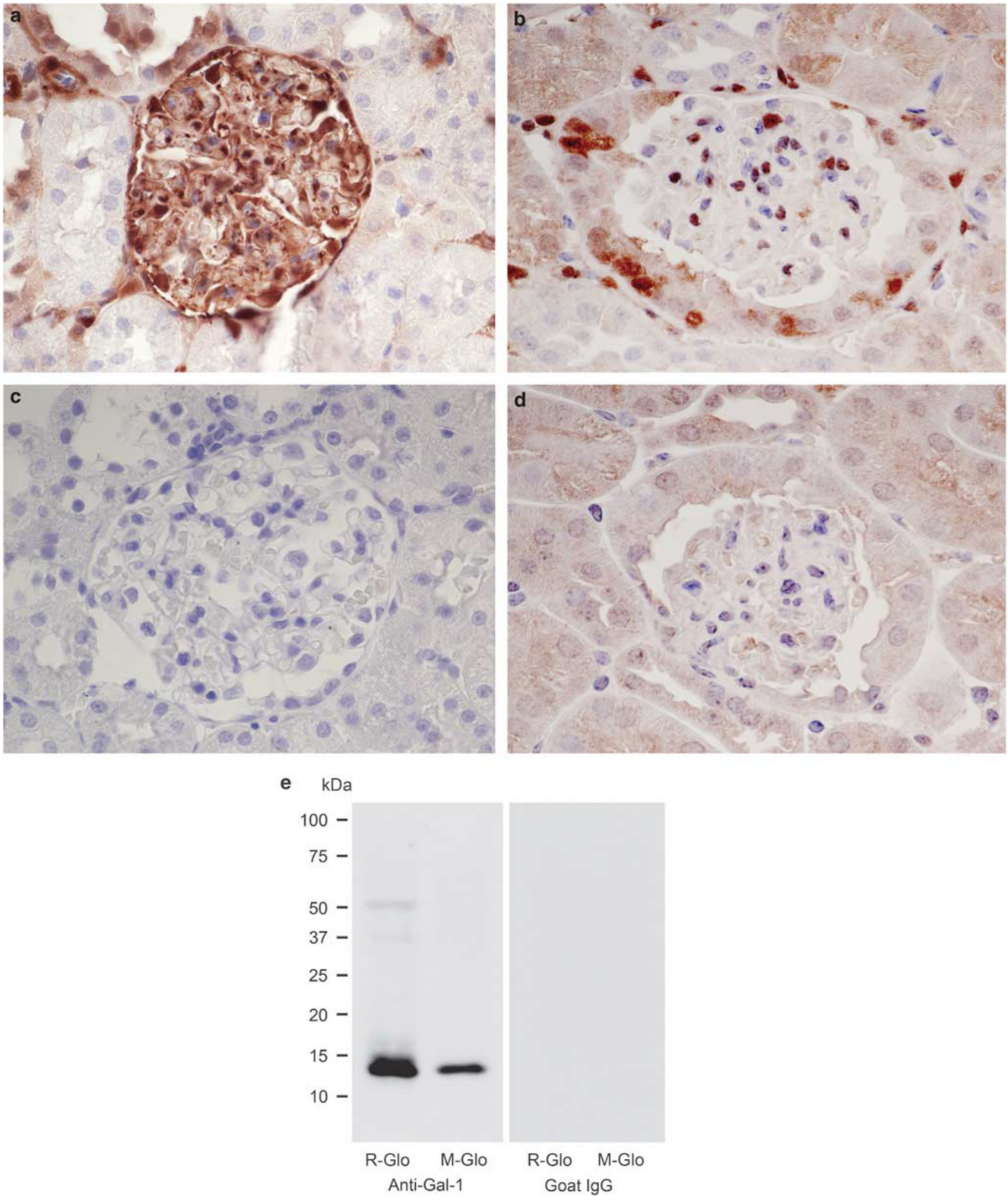

Figure 8 Distribution of Gal-1 in the rat (**a** and **c**) and mouse (**b** and **d**) normal glomerulus. The distribution pattern of Gal-1 in the rat was similar to that of human whereas mouse glomerulus demonstrated Gal-1 to be mainly in the mesangium and Bowman's epithelium. (**e**) Western blot study confirmed the specificity of the antibody used in the immunohistochemistry and the existence of Gal-1 protein in the rodent glomeruli.

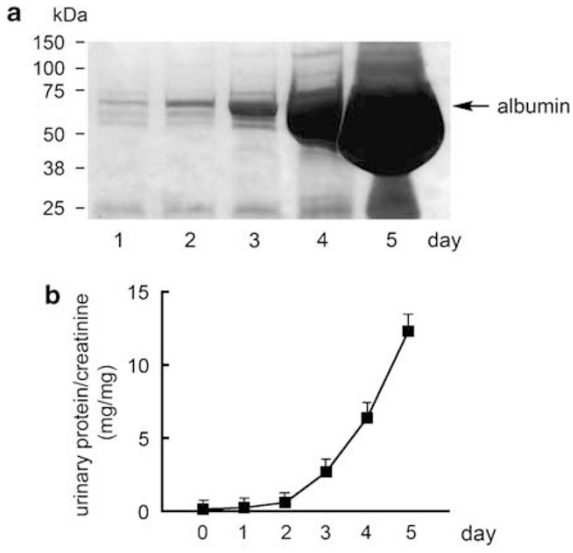

Figure 9 Proteinuria in puromycin aminonucleoside (PAN)-induced rat nephrosis. (**a**) Urine (10 μl) was loaded on a 5–20% gradient SDS–polyacrylamide gel electrophoresis and stained with Coomassie blue. (**b**) The amount of total urinary protein excretion was measured by the Bradford method and divided by creatinine.

did not show any positive staining in the same samples (Figure 8c and d). We further demonstrated the specificity of this antibody and the presence of Gal-1 protein in the isolated glomeruli of both rodents by Western blot analysis. In both cases, a 14-kDa protein band consistent with the Gal-1 monomer form was detected (Figure 8e). From these findings, we conclude that the two rodent systems are fundamentally different in terms of Gal-1 expression in the glomerulus. Thus, the lack of proteinuria in the Gal-1-deficient mouse[31] may be explained by the absence of Gal-1 expression in the mouse podocytes.

Reduced Expression of Nephrin and Gal-1 in PAN-Induced Nephrosis in Rats

The similar expression pattern of Gal-1 in the human and rat glomeruli prompted us to examine whether Gal-1 expression is also altered in PAN-induced nephrosis in rats, a well-accepted and widely used *in vivo* model of MCNS. PAN nephrosis was established in Sprague–Dawley rats, and the animals developed heavy proteinuria 3 days after the injection (Figure 9a and b). To study the involvement of Gal-1 alteration in the pathomechanism of the proteinuria, we focused on the expression of Gal-1, nephrin, and synaptopodin in the kidney samples around the onset of the proteinuria. The control rats not receiving PAN showed the distribution of Gal-1 to be clearly in the capillary wall as well as in the cytoplasm and the nucleus of podocytes (Figure 10). In the day-2 glomerulus, 1 day before significant proteinuria developed, the reduction in the amount of Gal-1 in the capillary wall was obvious; whereas there was no apparent change in Gal-1 in the day-1 glomerulus. In the day-3 glomerulus, Gal-1 expression was almost the same as that at day 2; whereas the day-5 glomerulus revealed a further reduction, especially in the podocyte cytoplasm. The change in nephrin expression tended to be similar to that in Gal-1; however, the apparent reduction in nephrin in the capillary wall was found at days 3 and 5 glomeruli. In contrast, there was no obvious difference in the expression of synaptopodin between the control glomerulus and PAN glomeruli. Western blot analysis showed that in the day-2 and day-5 glomeruli, there was a decrease in the amount of both nephrin isoforms, with the upper band being the plasma membrane form and lower band, the ER form.[4–6] More clearly, Gal-1 expression in the glomeruli at days 2 and 5 was drastically reduced (Figure 11).

Gal-1-Nephrin Interaction Induces Intracellular Signaling in Podocytes

Galectin-1 is known to be a potential signal transducer through binding to terminal glycans of several transmembrane glycoproteins.[32,33] To show the functional interaction of Gal-1 and nephrin, we next explored whether Gal-1 could induce intracellular signaling through binding to the ectodomain of nephrin. WT Gal-1 was added to cultures of a human podocyte cell line transiently transfected with a nephrin cDNA construct. We first examined the degree of intracellular tyrosine phosphorylation of nephrin. Base-line tyrosine phosphorylation of the nephrin cytoplasmic domain has been shown to be essential for cellular survival.[34] The base-line tyrosine phosphorylation was also seen in our nonstimulated nephrin-expressing cells (Figure 12a). However, once the cells had been stimulated for 1 h with recombinant Gal-1, a 1.7-fold (70%) increase in tyrosine phosphorylation of nephrin was observed (Figure 12a). The MAPK/ERK signaling cascade is regulated by a wide variety of upstream triggers involved in growth and differentiation, including receptor tyrosine kinases.[35] Also, Gal-1 triggers signaling pathways in hepatic stellate cells by activating mitogen-activated kinases MEK1/2-ERK1/2.[33] So next, we used immunoblotting to analyze cellular extracts derived from podocytes transiently transfected with a nephrin construct or vector only (control), with or without stimulation with Gal-1. Whereas both vector and nephrin-transfected cells contained ERK1/2 at similar levels, phospho-ERK was detected only in the nephrin-transfected cells with or without stimulation by Gal-1, indicating a relation between nephrin and activation of ERK1/2 in the nephrin-transfected cells (Figure 12b). However, in the nephrin-transfected podocytes, Gal-1-stimulation resulted in a 1.6-fold (60%) increase in phospho-ERK (Figure 12b). These data not only indicate that Gal-1 could induce intracellular signaling by stimulating ERK1/2, but also indicate that the presence of nephrin was essential for this signaling event, as phospho-ERK was not detected in vector-transfected cells stimulated with Gal-1 (Figure 12b, Vector + G1). To follow the early

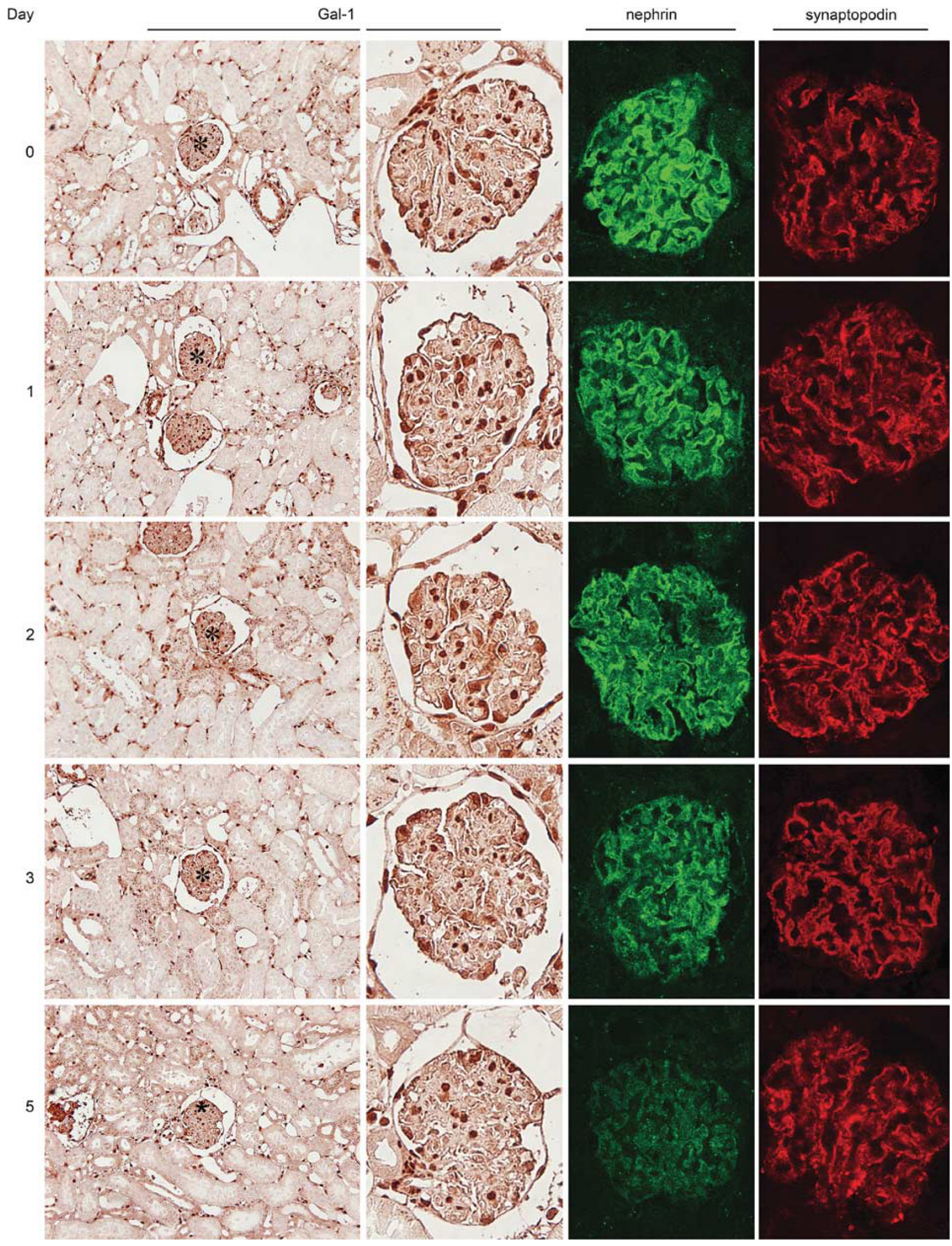

Figure 10 Expression of Gal-1, nephrin, and synaptopodin in PAN glomeruli. Immunohistochemistry by using paraffin-embedded sections was examined with Gal-1. Immunofluorescence and cofocal microscopy for nephrin and synaptopodin was examined by using the frozen sections and the frozen sections fixed with paraformaldehyde, respectively. The reduction of Gal-1 expression at the capillary tufts was apparently revealed in the glomerulus from the day 2-PAN glomerulus in parallel with that of nephrin. In contrast, there was no obvious reduction with synaptopodin expression through 5 days after injection of PAN.

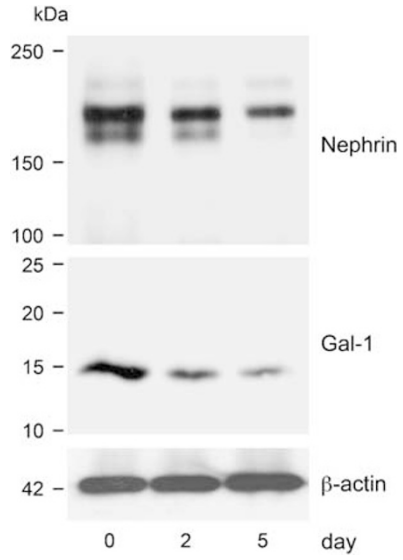

Figure 11 Protein expression of Gal-1 and nephrin in PAN glomeruli. Protein lysate (30 μg) from isolated glomeruli were subjected to SDS–PAGE and western blot analysis with nephrin, Gal-1, and β-actin. The apparent reduction of Gal-1 and nephrin was observed in the glomeruli already at day 2 after PAN injection.

kinetics of this signaling event, we further performed a time-course experiment by following the progression of ERK1/2 phosphorylation in Gal-1-stimulated, nephrin-transfected cells up to 120 min. The data showed that phosphorylation of ERK1/2 peaked (twofold above background) at 10 min after stimulation with Gal-1 and remained elevated (1.6-fold) for at least 120 min (Figure 12c).

DISCUSSION

In the present study, we found for the first time that Gal-1 is possibly a new extracellular ligand for nephrin at the glomerular SD in the human and rat kidney, but not in the mouse kidney. We showed that Gal-1 is synthesized by podocytes and that its expression is decreased in parallel to that of nephrin in patients with MCNS and in the rat model of MCNS. Our clinical data point to a close association between the reduced expression of both Gal-1 and nephrin and the heavy proteinuria in the glomerulus during the heavy proteinuric state.

Compelling evidence highlights the critical role of nephrin in the maintenance of perm-selective barrier;[1] however, little is known about the complex inter- and intramolecular interactions between nephrin and other components of the SD. Among all the proteins identified at the SD, only NEPH1[36] and NEPH2[37] have thus far been shown to directly interact with the ectodomain of nephrin. Similar to nephrin, NEPH1 and NEPH2 are also type-1 transmembrane glycoproteins of the immunoglobulin super family, having extracellular immunoglobulin-like domains with *N*-linked glycosylation. In the present study, we focused only on the Gal-1 and nephrin interaction. Our data herein showing colocalization and binding capacity between Gal-1 and nephrin could reveal direct interaction of Gal-1 with β-galactosides of nephrin; however, as β-galactosides are the major site of recognition for Gal-1, it is most likely that this dimeric lectin would also bind to other *N*-linked glycans at the SD and introduce inter- and intramolecular interactions. Thus, it is tempting to speculate that Gal-1 is secreted by podocytes, either as a free molecule or in complex with its interacting SD components, and may contribute to the structural and functional stability of the SD by organizing and interconnecting nephrin and other transmembrane glycoproteins at the SD.

Temporal and spatial expression of Gal-1 is developmentally regulated differently among different species. For instance, Gal-1 is expressed in the developing rat brain but not in the adult brain.[38] Our present study clearly revealed a fundamental difference in the expression of Gal-1 in the mouse glomerulus as compared with that in human and rat ones. The lack of Gal-1 in the mouse podocytes and the capillary wall is a reasonable explanation for the lack of kidney phenotype and proteinuria in the Gal-1-deficient mouse.[31] This explanation is in perfect agreement with our finding that both human and rat showed similar localization of Gal-1 in the normal glomerulus and that both species also revealed a reduction in Gal-1 expression during proteinuria. Furthermore, we found that the reduction in the Gal-1 expression in patients with MCNS and rats with PAN-induced nephrosis is closely associated with a reduction in nephrin expression and staining at the SD. An immediate implication of this finding is that, despite similarities in the structure and components of the SD reported in humans and mice, there may still be fundamental differences to be discovered between these two species.

Human Gal-1 exists as a homodimer in solution, the integrity of which is maintained and stabilized through a conserved hydrophobic core located at the dimer interface.[39] However, it has been reported that the homodimer is dissociated into monomers at lower concentrations (7 μM),[40] whereas still retaining its β-galactoside-binding properties.[41] Our kinetic studies using a BIAcore biosensor were carried out using samples of Gal-1 in the lower concentration range (0.25–2 μM), indicating that Gal-1 was mostly in its monomeric form while interacting with the immobilized nephrin. This is consistent with our global curve-fit analysis, which was best fitted to a simple 1:1 interaction model with a conformational change. The change in conformation is most likely reflecting a transition in binding, as shown by the rapid primary association and dissociation phases of the sensorgrams. A similar transient and rapid interaction pattern was also reported for binding of Gal-1 to the cell-surface glycoproteins CD45 and Thy-1.[42] Interestingly, our calculated affinity binding constant for Gal-1-nephrin interaction ($K_D \sim 1.7\,\mu$M) is within the range of what it was reported for CD45[42] ($K_D \sim 5\,\mu$M), and also for laminin ($K_D \sim 1\,\mu$M),[43]

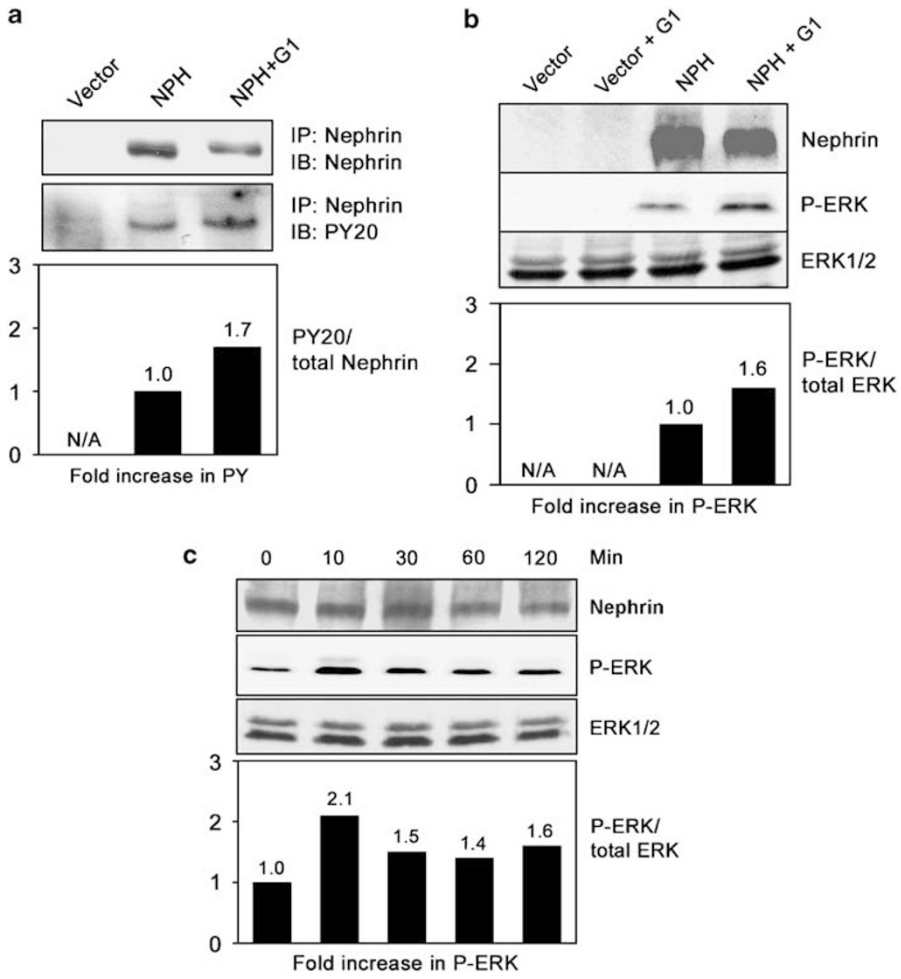

Figure 12 Phosphorylation study by Gal-1-nephrin interaction. (**a**) Western blot study showing increased tyrosine phosphorylation of nephrin after stimulation with Gal-1. Podocytes were transfected with vector only (vector) and with nephrin (NPH) before stimulation and after stimulation (NPH + G1) with recombinant Gal-1 for 1 h. Immunoprecipitation (IP) was performed with anti-NPH antibody and change in the levels of tyrosine phosphorylation was visualized by immunoblotting (IB) using anti-phosphotyrosine antibody (PY20). Bars in the lower graph show a 1.7-fold increased phosphorylation of NPH (PY20/total NPH) after stimulation with Gal-1. The base-line phosphorylation in the nonstimulated NPH-transfected sample is set as 1 for comparison. (**b**) Activation of ERK1/2 through Gal-1-NPH interaction. Middle panel shows the levels of ERK1/2 phosphorylation (P-ERK). Lower panel shows total levels of ERK1/2. Graph shows fold increase in ERK1/2 phosphorylation (P-ERK/total ERK). (**c**) Time-course analysis of ERK1/2 phosphorylation in nephrin-transfected cells stimulated with Gal-1 for 0, 10, 30, 60, and 120 min. Graph shows a peak of twofold increased in P-ERK at 10 min after stimulation.

indicating that Gal-1 may recognize and interact with the same carbohydrate structure attached to these molecules.

Galectin-1 can be found intracellularly, extracellularly, as well as at the cell surface; and its functions seem to vary depending on its location.[30] For example, intracellular Gal-1 has been shown to play a role in cell-cycle, RNA splicing, and transcriptional regulation; whereas extracellular and cell-surface-bound Gal-1's are involved in cell–cell and cell–matrix interactions, immune response, apoptosis, and neoplastic transformation.[30,44,45] It was previously reported that Gal-1 induces signaling pathways of hepatic stellate cells through activating mitogen-activated kinases MEK1/2-ERK1/2.[33] Gal-1 is also known to trigger tyrosine phosphorylation of phospholipase Cγ1[46] that in turn induces ERK activation. Our data clearly indicate that upon binding to nephrin, Gal-1 can also trigger increased tyrosine phosphorylation of nephrin, resulting in the induction of ERK activation. What cellular process is followed after ERK-activation through interaction with nephrin in the mature podocytes, however, remains to be investigated. Nonetheless, it is reasonable to consider that alteration of proper signaling pathways at the SD contributes not only to the pathological status such as proliferation, apoptosis, and cellular activation but also to maintaining the cell viability under the static condition without prominent intracellular activation. Therefore, it is tempting to speculate that Gal-1 plays a role in maintaining the podocyte viability through interaction with nephrin and most likely with other SD-glycoproteins such as NEPH1 and NEPH2.

In the present study, we also found Gal-3 to be present in the human glomerulus, expressed in the endothelium, but not in the podocyte. This result seems to be reasonable

because previous study using this antibody identified Gal-3 also to be localized in the endothelium of normal human liver.[18] In addition, Gal-3 immunostaining was clearly positive in the glomerular endothelium of a rat ischemic model at the late stage after reperfusion.[47] Another previous study also found Gal-3 to be present in the glomerular mesangium in rat Thy-1.1 glomerulonephritis.[48] In the present study, the results of our Western blot experiment using protein samples of glomeruli highly isolated from human kidney strengthen the existence of Gal-3 protein in the glomerular endothelium that was revealed by our immunohistochemistry. Whether Gal-3 is produced by the endothelium remains to be elucidated. Gal-3 is produced by many tissues such as lung and peripheral blood cells.[49] Thus, one could also speculate that soluble Gal-3 secreted by many tissues may bind to the glomerular endothelium by interacting with the abundant glycoproteins called the glycocalyx.[1] Indeed, it is known that Gal-3 is a receptor that acts against advanced glycation end products in the endothelium and that Gal-3-deficient mice have accelerated diabetic glomerulopathy[50] All of our kidney samples were from adult patients, whereas a previous study showing Gal-3 expression in human normal kidney was examined by using infant kidney.[15] It would be of interest to study how Gal-3 expression in the glomerular endothelium alters in parallel with aging and whether Gal-3 is strongly expressed in the glomerular endothelium in the diabetic kidney.

In conclusion, we have demonstrated that Gal-1 is a new extracellular ligand of nephrin at the SD and may play a role in the crucial function of the SD by participating in and organizing the molecular interactions of nephrin with itself and with other SD components. Additional experiments to study possible interaction of Gal-1 with other SD components such as NEPH and NEPH2 should be required to explore further biological implication of Gal-1 in the integrity of the SD function and the podocyte biogenesis.

ACKNOWLEDGEMENTS

We thank Ms S Matsubara for the excellent technical assistance with electron microscopy. This study was supported by the Promotion and Mutual Aid Corporation for Private Schools of Japan and Novartis Pharma (KK).

1. Tryggvason K, Patrakka J, Wartiovaara J. Hereditary proteinuria syndromes and mechanisms of proteinuria. New Engl J Med 2006;354:1387–1401.
2. Lenkkeri U, Mannikko M, McCready P, *et al.* Structure of the gene for congenital nephrotic syndrome of the Finnish type (NPHS1) and characterization of mutations. Am J Hum Genet 1999;64:51–61.
3. Khoshnoodi J, Hill S, Tryggvason K, *et al.* Identification of *N*-linked glycosylation sites in human nephrin using mass spectrometry. J Mass Spectrom 2007;42:370–379.
4. Yan K, Khoshnoodi J, Ruotsalainen V, *et al. N*-linked glycosylation is critical for the plasma membrane localization of nephrin. J Am Soc Nephrol 2002;13:1385–1389.
5. Fujii Y, Khoshnoodi J, Takenaka H, *et al.* The effect of dexamethasone on defective nephrin transport caused by ER stress: a potential mechanism for the therapeutic action of glucocorticoids in the acquired glomerular diseases. Kidney Int 2006;69:1350–1359.
6. Nakajo A, Khoshnoodi J, Takenaka H, *et al.* Mizoribine corrects defective nephrin biogenesis by restoring intracellular energy balance. J Am Soc Nephrol 2007;18:2554–2564.
7. Perillo NL, Marcus ME, Baum LG. Galectins: versatile modulators of cell adhesion, cell proliferation, and cell death. J Mol Med 1998;76:402–412.
8. Hughes RC. Galectins in kidney development. Glycoconj J 2004;19:621–629.
9. Hadari YR, Paz K, Dekel R, *et al.* Galectin-8. A new rat lectin, related to galectin-4. J Biol Chem 1995;270:3447–3453.
10. Wada J, Ota K, Kumar A, *et al.* Developmental regulation, expression, and apoptotic potential of galectin-9, a beta-galactoside binding lectin. J Clin Invest 1997;99:2452–2461.
11. Camby I, Le Mercier M, Lefranc F, *et al.* Galectin-1: a small protein with major functions. Glycobiology 2006;16:137R–157R.
12. Hirabayashi J, Ayaki H, Soma G, *et al.* Production and purification of a recombinant human 14 kDa beta-galactoside-binding lectin. FEBS Lett 1989;250:161–165.
13. Hirabayashi J, Kawasaki H, Suzuki K, *et al.* Further characterization and structural studies on human placenta lectin. J Biochem 1987;101:987–995.
14. Elola MT, Wolfenstein-Todel C, Troncoso MF, *et al.* Galectins: matricellular glycan-binding proteins linking cell adhesion, migration, and survival. Cell Mol Life Sci 2007;64:1679–1700.
15. Winyard PJ, Bao Q, Hughes RC, *et al.* Epithelial galectin-3 during human nephrogenesis and childhood cystic diseases. J Am Soc Nephrol 1997;8:1647–1657.
16. Van den Brule FA, Fernandez PL, Buicu C, *et al.* Differential expression of galectin-1 and galectin-3 during first trimester human embryogenesis. Dev Dyn 1997;209:399–405.
17. Ostalska-Nowicka D, Zachwieja J, Nowicki M, *et al.* Immunohistochemical detection of galectin-1 in renal biopsy specimens of children and its possible role in proteinuric glomerulopathies. Histopathology 2007;51:468–476.
18. Shimonishi T, Miyazaki K, Kono N, *et al.* Expression of endogenous galectin-1 and galectin-3 in intrahepatic cholangiocarcinoma. Hum Pathol 2001;32:302–310.
19. Ruotsalainen V, Reponen P, Khoshnoodi J, *et al.* Monoclonal antibodies to human nephrin. Hybrid Hybridomics 2004;23:55–63.
20. Nakatsue T, Koike H, Han GD, *et al.* Nephrin and podocin dissociate at the onset of proteinuria in experimental membranous nephropathy. Kidney Int 2005;67:2239–2253.
21. Khoshnoodi J, Sigmundsson K, Ofverstedt LG, *et al.* Nephrin promotes cell-cell adhesion through homophilic interactions. Am J Pathol 2003;163:2337–2346.
22. Hirabayashi J, Kasai K. Effect of amino acid substitution by sited-directed mutagenesis on the carbohydrate recognition and stability of human 14-kDa beta-galactoside-binding lectin. J Biol Chem 1991;266:23648–23653.
23. Nishibori Y, Liu L, Hosoyamada M, *et al.* Disease-causing missense mutations in NPHS2 gene alter normal nephrin trafficking to the plasma membrane. Kidney Int 2004;66:1755–1765.
24. Kataoka S, Kudo A, Hirano H, *et al.* 11 beta-hydroxysteroid dehydrogenase type 2 is expressed in the human kidney glomerulus. J Clin Endocrinol Metab 2002;87:877–882.
25. Yan K, Kudo A, Hirano H, *et al.* Subcellular localization of glucocorticoid receptor protein in the human kidney glomerulus. Kidney Int 1999;56:65–73.
26. Takemoto M, Asker N, Gerhardt H, *et al.* A new method for large scale isolation of kidney glomeruli from mice. Am J Pathol 2002;161:799–805.
27. Delarue F, Virone A, Hagege J, *et al.* Stable cell line of T-SV40 immortalized human glomerular visceral epithelial cells. Kidney Int 1991;40:906–912.
28. Hosoyamada M, Yan K, Nishibori Y, *et al.* Nephrin and podocin expression around the onset of puromycin aminonucleoside nephrosis. J Pharmacol Sci 2005;97:234–241.
29. Khoshnoodi J, Sigmundsson K, Cartailler JP, *et al.* Mechanism of chain selection in the assembly of collagen IV: a prominent role for the alpha2 chain. J Biol Chem 2006;281:6058–6069.
30. Elola MT, Chiesa ME, Alberti AF, *et al.* Galectin-1 receptors in different cell types. J Biomed Sci 2005;12:13–29.
31. Poirier F, Robertson EJ. Normal development of mice carrying a null mutation in the gene encoding the L14 S-type lectin. Development 1993;119:1229–1236.

32. Sacchettini JC, Baum LG, Brewer CF. Multivalent protein-carbohydrate interactions. A new paradigm for supermolecular assembly and signal transduction. Biochemistry 2001;40:3009–3015.
33. Maeda N, Kawada N, Seki S, *et al.* Stimulation of proliferation of rat hepatic stellate cells by galectin-1 and galectin-3 through different intracellular signaling pathways. J Biol Chem 2003;278:18938–18944.
34. Huber TB, Kottgen M, Schilling B, *et al.* Interaction with podocin facilitates nephrin signaling. J Biol Chem 2001;276:41543–41546.
35. Pearson G, Robinson F, Beers Gibson T, *et al.* Mitogen-activated protein (MAP) kinase pathways: regulation and physiological functions. Endocr Rev 2001;22:153–183.
36. Gerke P, Huber TB, Sellin L, *et al.* Homodimerization and heterodimerization of the glomerular podocyte proteins nephrin and NEPH1. J Am Soc Nephrol 2003;14:918–926.
37. Gerke P, Sellin L, Kretz O, *et al.* NEPH2 is located at the glomerular slit diaphragm, interacts with nephrin and is cleaved from podocytes by metalloproteinases. J Am Soc Nephrol 2005;16:1693–1702.
38. Joubert R, Kuchler S, Zanetta JP, *et al.* Immunohistochemical localization of a beta-galactoside-binding lectin in rat central nervous system. I. Light- and electron-microscopical studies on developing cerebral cortex and corpus callosum. Dev Neurosci 1989;11: 397–413.
39. Lopez-Lucendo MF, Solis D, Andre S, *et al.* Growth-regulatory human galectin-1: crystallographic characterisation of the structural changes induced by single-site mutations and their impact on the thermodynamics of ligand binding. J Mol Biol 2004;343:957–970.
40. Cho M, Cummings RD. Galectin-1, a beta-galactoside-binding lectin in Chinese hamster ovary cells. I. Physical and chemical characterization. J Biol Chem 1995;270:5198–5206.
41. Leppanen A, Stowell S, Blixt O, *et al.* Dimeric galectin-1 binds with high affinity to alpha2,3-sialylated and non-sialylated terminal N-acetyllactosamine units on surface-bound extended glycans. J Biol Chem 2005;280:5549–5562.
42. Symons A, Cooper DN, Barclay AN. Characterization of the interaction between galectin-1 and lymphocyte glycoproteins CD45 and Thy-1. Glycobiology 2000;10:559–563.
43. Zhou Q, Cummings RD. The S-type lectin from calf heart tissue binds selectively to the carbohydrate chains of laminin. Arch Biochem Biophys 1990;281:27–35.
44. Camby I, Le Mercier M, Lefranc F, *et al.* Galectin-1: a small protein with major functions. Glycobiology 2006;16:137–157.
45. Rabinovich GA, Baum LG, Tinari N, *et al.* Galectins and their ligands: amplifiers, silencers or tuners of the inflammatory response? Trends Immunol 2002;23:313–320.
46. Walzel H, Blach M, Hirabayashi J, *et al.* Involvement of CD2 and CD3 in galectin-1 induced signaling in human Jurkat T-cells. Glycobiology 2000;10:131–140.
47. Nishiyama J, Kobayashi S, Ishida A, *et al.* Up-regulation of galectin-3 in acute renal failure of the rat. Am J Pathol 2000;157:815–823.
48. Sasaki S, Bao Q, Hughes RC. Galectin-3 modulates rat mesangial cell proliferation and matrix synthesis during experimental glomerulonephritis induced by anti-Thy1.1 antibodies. J Pathol 1999;187:481–489.
49. Dumic J, Dabelic S, Flögel M. Galectin-3: an open-ended story. Biochim Biophys Acta 2006;1760:616–635.
50. Pugliese G, Pricci F, Iacobini C, *et al.* Accelerated diabetic glomerulopathy in galectin-3/AGE receptor 3 knockout mice. FASEB J 2001;15:2471–2479.